Some solutions for online monitoring the vibration of transformers and the application to identify the state of the transformers

Tran Thu Hang, Dao Duy Yen
Thai Nguyen University of Technology, Thai Nguyen Province, Vietnam.
Corresponding author: Truong Tuan Anh, e-mail: truongtuananh@tnut.edu.vn
This research is funded by Thai Nguyen University of Technolsogy, Vietnam

Abstract

The electrical system is a complex system in both structure and operation. When an incident occurs, any element of the system affects the reliability of electricity supply, electricity quality and causes great damage to economy. The identification the state of transformers in the working process will help us diagnose early the breakdown forms in the 3-phase transformers. This is a necessary work because it will contribute to reduce economic losses and improve the reliability, the quality of electricity supplied to consumers. The paper focuses on research some solutions for online monitoring the vibration of transformers and application to identify the state of the transformers distributaring at 22/0.4kV in normal working condition and in 6 breakdown form.

Keywords: *Detection of incident, transformer model, ANSYS software, the finite element method, winding.*

1. INTRODUCTION

Currently, there are many methods to monitor the state of transformers: (1) Dissolve Gas Analysis (DGA), (2) Measurements of Partial Discharge in transformers (PD), (3) Frequency Response Analysis (FRA). The paper will focus on the method of analysis of response frequency to monitor and diagnose the state of the MBA.

2. ANALYSE THE DOMAIN OF VIBRATION FREQUENCY

The loss of the original mechanical feature of the force transformers as the deformation of the winding, the displacement of the steel core,… is caused by great electromechanical forces. The cause of this phenomenon is the fault current. If the deformation of the winding and the displacement of the steel core are not detected early they will turn into a heat and dielectric failure. The types of damage are immutable and can only be repaired by an overhaul of the transformers such as rewinding the winding, repairing the steel core or completed replacing the transformers. Therefore, we need to check the mechanical integrity of newly installed transformers periodically after the transport process or operating, and especially after short-circuit problems to assess abnormal conditions and provide early warning of possible damage. For more than a decade, the manufacturers of transformers around the world have come up with and applied a new technique to solve effectively this problem. It is named "Frequency Response Analysis technique" (FRA).

2.1. The basis of frequency response

The transformer is considered a complex network of RLC elements. The contributions to this RLC complex network come from the resistance of the copper coil; the inductance of the windings and the capacitance coming from the insulating layers among the windings, between the winding and the winding, between the winding and the steel core, between the steel core and case, between the case and the winding. However, we can use a simplified isotropic circuit with the aggregated RLC elements (illustrated in Figure 1) to explain accurately the principle of frequency response technique.

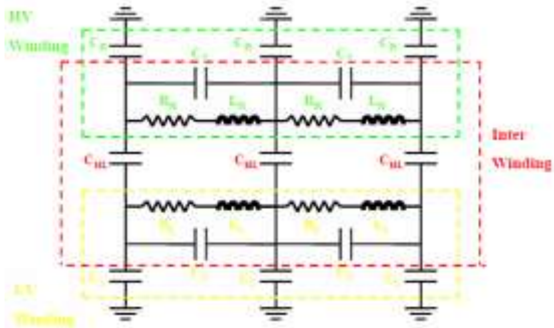

Figure 1. The simplified isotropic circuit with the aggregated RLC elements

The frequency response is carried out by applying a low voltage signal with variable frequencies into the windings of transformer and measuring both input and output signals. The ratio of these two signals gives us the required response. This ratio is called the transfer function of the transformer. So we can obtain values of its magnitude and phase angle. With different frequencies, the RLC network will give different impedance circuits. Therefore, the transmission function at each frequency is a unit of measurement of the actual impedance of RLC network of the transformer.

3. OVERVIEW OF VIBRATION PHENONMENON IN TRANSFORMER

The vibration in the transformer is generated by different forces that appear in the steel core and the coil inside the transformer during operation.

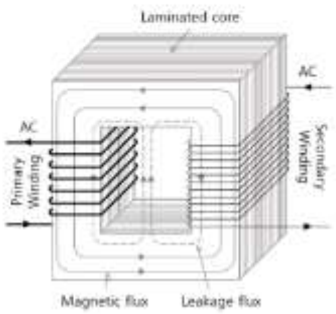

Figure 2: Magnetic circuit and winding of the transformer

The vibration in the winding is caused by electrodynamic force when there is an interaction between the current flowing in the winding and the magnetic flux probe. This force is proportional to the square of the current and consists of the axial and radial components.

The vibration of the steel core is due to a phenomenon called magnetism that occurs when the metal objects are placed in a magnetic field and are deformed.

4. THE ANALYSIS OF VARIABLE FREQUENCY RESPONSE OF TRANSFORMER IN NORMAL AND INCIDENCE WORKING MODE BY ANSYS SOFTWARE

In this paper, the author will perform the simulations and data processing as follows:

- Code A: Transformer works normally.
- Code B: Transformer is convoluted two wires.
- Code C: Transformer is convoluted 5% of the total number of high-voltage windings.
- Code D: Transformer is convoluted 10% of the total number of high-voltage windings.

4.1. The vibration results of the transformer in the working modes

4.1.1. Transformer works normally

The displacement in the x-direction of the case.

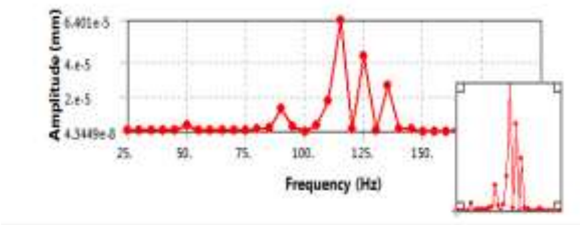

Figure 3. The displacement in the x-direction of the case

The maximum amplitude reaches 6,401.10-5mm with frequency 115Hz.

The displacement in the y-direction of the case.

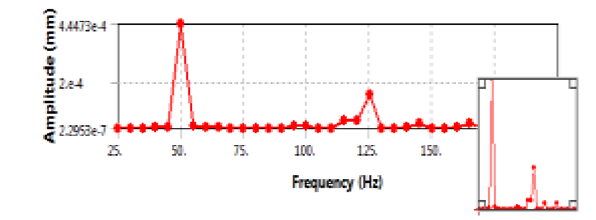

Figure 4. The displacement in the y-direction of the case

The largest displacement in the y- direction is 4,4473.10-5mm, corresponding to the frequency of 50 Hz.

The displacement in the z-direction of the case.

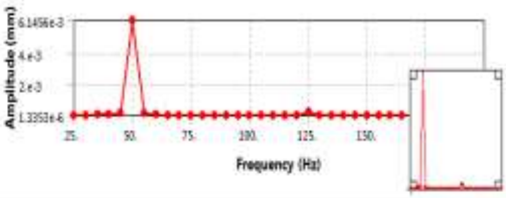

Figure 5. The displacement in the z-direction of the case

The largest displacement in the z- direction is 6.1410^{-5}mm, corresponding to the frequency of 50 Hz.

4.1.2. Code B: Transformer is convoluted two wires

The displacement in the x-direction of the case.

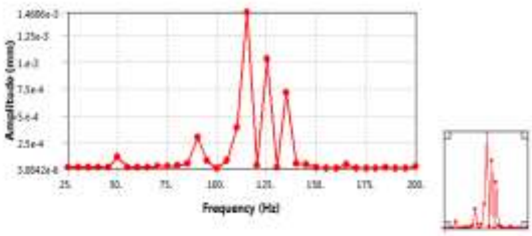

Figure 6. The displacement in the x-direction of the case

The maximum amplitude reaches 0.00146mm with frequency 120Hz.

The displacement in the y-direction of the case.

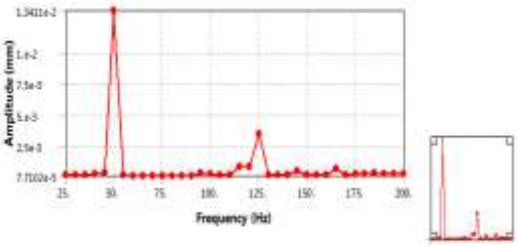

Figure 7. The displacement in the y-direction of the case

The largest displacement in the y- direction is 0.0134mm, corresponding to the frequency of 50 Hz.

The displacement in the z-direction of the case.

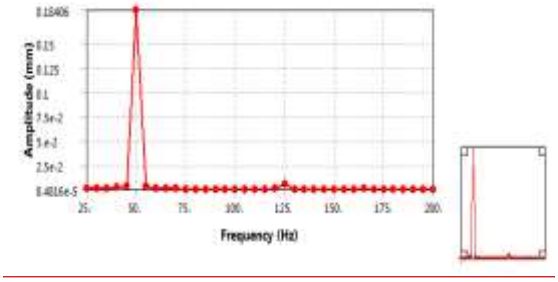

Figure 8. The displacement in the z-direction of the case

The largest displacement in the z- direction is 0.18406mm, corresponding to the frequency of 50 Hz.

4.1.3. Code C: Transformer is convoluted 5% of the total number of high-voltage windings

The displacement in the x-direction of the case.

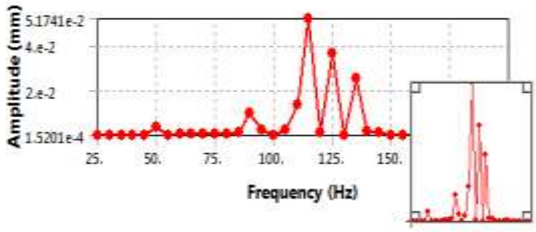

Figure 9. The displacement in the x-direction of the case

The largest displacement in the x- direction is 0.051741mm, corresponding to the frequency of 120 Hz.

The displacement in the y-direction of the case.

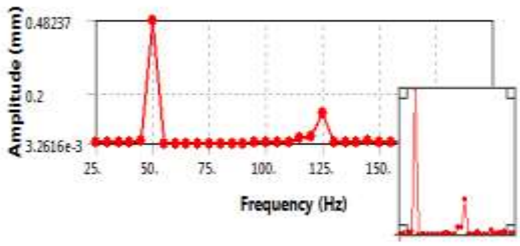

Figure 10. The displacement in the y-direction of the case

The largest displacement in the y- direction is 0.48237mm, corresponding to the frequency of 50Hz.

The displacement in the z-direction of the case.

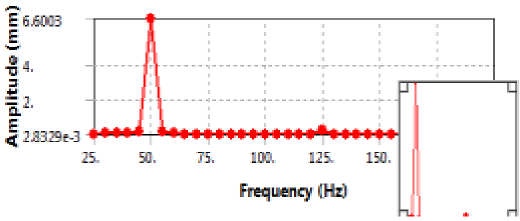

Figure 11. The displacement in the z-direction of the case

The largest displacement in the z- direction is 6.6mm, corresponding to the frequency of 50Hz.

4.1.4. Code D: Transformer is convoluted 10% of the total number of high-voltage windings

The displacement in the x-direction of the case.

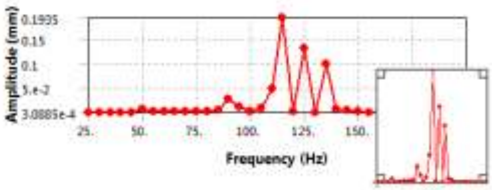

Figure 12. The displacement in the x-direction of the case

The largest displacement in the x- direction is 0.1935mm, corresponding to the frequency of 120Hz.

The displacement in the y-direction of the case.

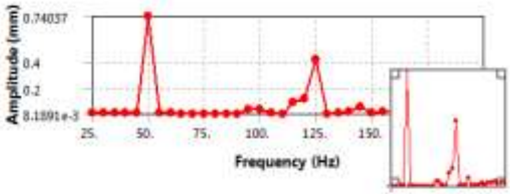

Figure 13. The displacement in the y-direction of the case

The largest displacement in the y- direction is 0.74037mm, corresponding to the frequency of 50Hz.

The displacement in the z-direction of the case.

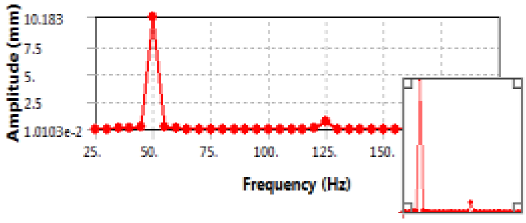

Figure 14. The displacement in the z-direction of the case

The largest displacement in the z- direction is 10.183mm, corresponding to the frequency of 50Hz.

5. DESIGN THE VIBRATION MONITORING DEVICES OF THE TRANSFORMER

5.1. Acceleration sensor

5.1.1. Introduce about acceleration sensor

MEMS sensor is a micro-electromechanical sensor system. It is manufactured by micro-electromechanical technology with two types of capacitors and resistive sensor. The type of resistive sensor has a simple construction, but its operation is highly dependent on temperature changes and is less sensitive than a capacitor sensor. In contrast, the type of capacitor sensor has a higher sensitivity, less dependent on temperature changes, less noise, less energy loss but it has complex electronic circuits. Currently, The type of capacitor acceleration sensor is the most widely used type.

Figure 15. The type of capacitor acceleration sensor

5.1.2. Select accelerometer sensor

In the article, the author chose a popular sensor, InvenSense's MPU-6050. This sensor is using the communication standard I2C. MPU-6050 is one of the first motion sensor system solutions in the world with up to 6 (expandable to 9) integrated sensor axes in a single chip. Depending on the requirements, the MPU-6050 sensor can operate in high-speed processing mode or in accurate (slower) angle measurement mode. MPU-6050 is capable of measuring in the range of gyroscope (±250; ±500; ±1000; ±2000 dps) and acceleration (±2; ±4; ±8; ±16g).

The MPU-6050 has a data buffer, 1024-byte, that allows the microcontroller issues commands to the sensor, and receive data after the MPU-6050 calculating finishly.

5.1.3. The diagram of the measuring system

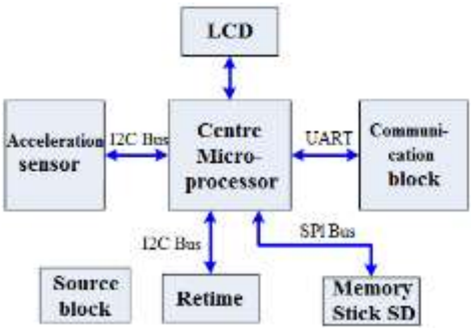

Figure 16. The diagram of the measuring system

5.1.4. Printed circuit

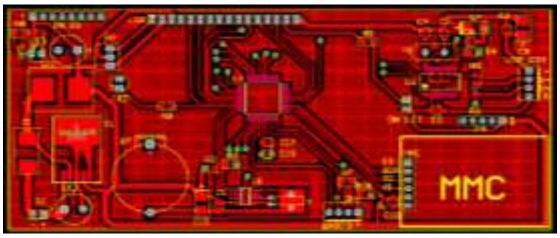

The above-side of printed circuit.

Figure 17. The above-side of printed circuit

The under-side of printed circuit.

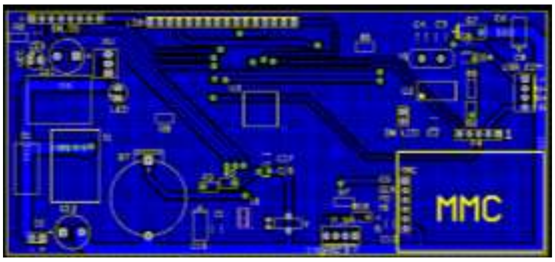

Figure 18. The under-side of printed circuit

5.1.5. Algorithm flowchart of microprocessor and acceleration sensor

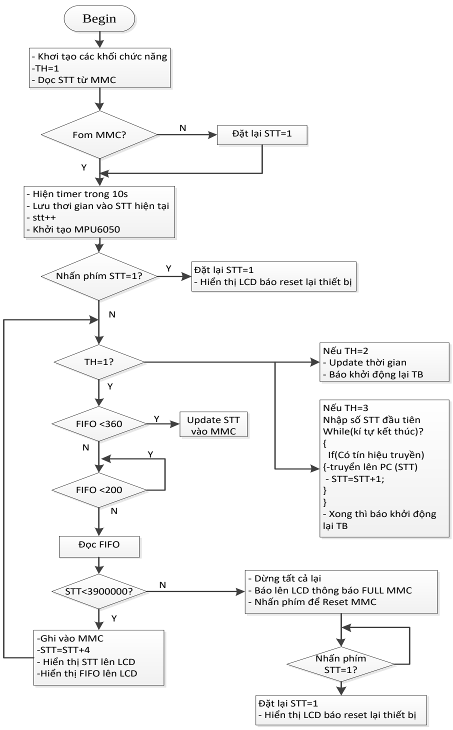

Figure 19. Algorithm flowchart of microprocessor and acceleration sensor

6. SOME RESULT OF IMPLEMENTATION AND TESTING

6.1. Hardware

The hardware includes 2 blocks: Sensor block and micro-processor block.

- **Sensor block:** The sensor block is designed to be in a closed box shown in Figure 20.

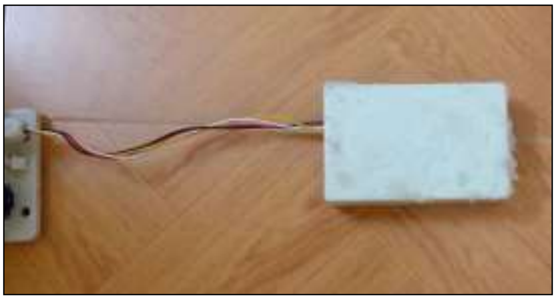

Figure 20. Sensor block

The sensor block mounted on the side of the device, is used to measure the vibration of the transformer and transfer data to memory.

- The Micro-processor block: It is designed to be in a closed box shown in Figure 21.

Figure 21. The Micro-processor block

6.2. The microprocessor software

Using software PsocDesigner of InvenSense 5.3 to write programs for microprocessor PSoC CY8C29566. The microprocessor reads data continuously from the sensor and sends it to the memory card SD.

7. CONCLUSION AND RECOMMENDATIONS

The article has built a model of the transformer 400kVA 22-0.4kV Y-Y0 by ANSYS software and and simulated the results of the current characteristics, the phase of voltage, the electromagnetic forces applied to the windings when the transformer works normally and the transformer is convoluted two wires.

The next development direction of the paper is to study the vibration frequency response on the shell of transformer in normal and faulty working mode [9], [10]. Some results of the survey and the initially calculating as follows the figure 22.

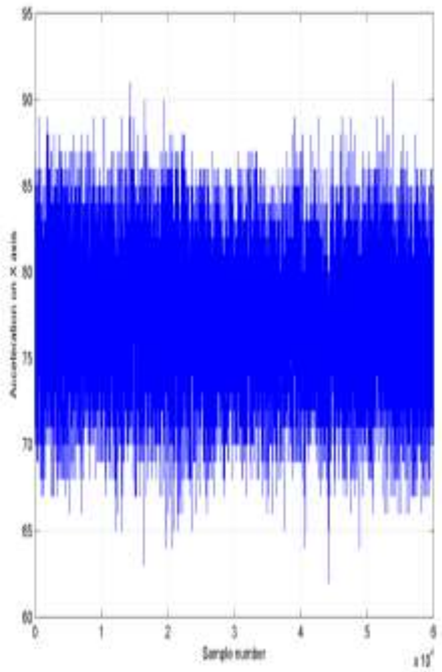

Figure 22. The signal is obtained from the accelerometer (x-axis) in 1 minute

Figure 22 is the result of signal collecting from the acceleration sensor within a minute on the x-axis. The results show that the acceleration sensor is quite sensitive so the vibration signal (acceleration) along the x-axis varies quite clearly during monitoring time. With the sampling frequency of the accelerometer sensor is $f_s = 1000Hz = 1kHz$, According to Nyquist's theorem, when analyzing the Fourier spectrum of the signal, we can detect up to frequency $f_s / 2 = 500Hz$. Calculating the amplitude spectrum of the signal in figure 22, we get the results shown in figure 23.

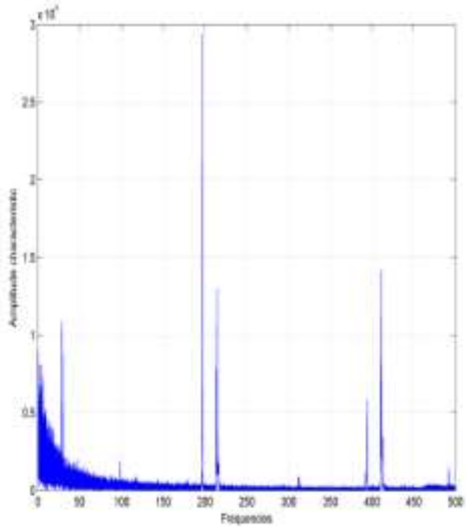

Figure 23. The amplitude spectrum characteristic of a signal window inn 60s

From the results of spectral characteristics analysis shown in figure 23, we see clearly the top of spectrum at 30Hz, small spectrum top at 100Hz and large spectrum top near of 200Hz, 210Hz, 400Hz and 420Hz. This result is relatively consistent with the theoretical that the transformer will vibrate at twice of the frequency of the electrical signal frequency ($2\times 50 = 100$ Hz) and the harmonics of this frequency. The result is quite different from the vibration frequency at 30Hz. We can temporarily assume that this is the main vibration frequency of the mechanical structure of the transformer. Besides, the high harmonic of this frequency is also observed at 210Hz and 420Hz. To investigate the repetition of this observations and comments on the top of the frequency spectrum, we will analyze and determine the top of spectrum for all segments in one minute in the signal (196 consecutive segments have been collected) and the results are shown in figure 24.

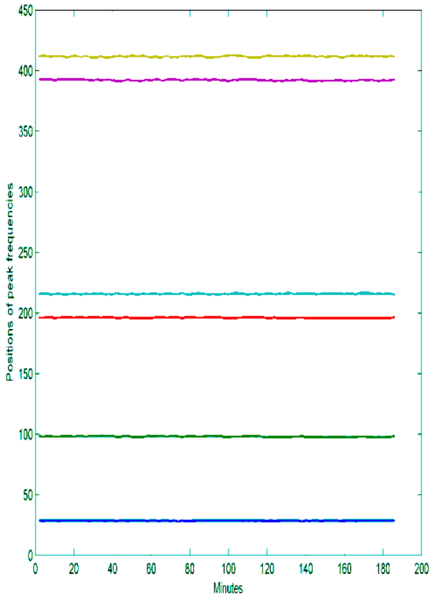

Figure 24: The graph of changes of the top of spectrum with measurement time

REFERENCES

1. *Phan Tu Thu (2005), The design of power transformers, The Scientific and Technical Publishing.*

2. Department of Electrical Machines and Electric Devices (1967), The design of power transformers, Hanoi University of Science and Technology Publishing.

3. S. Brahma (2005), Fault location scheme for a multi-terminal transmission line using synchronized voltage measurements, IEEE Trans. Power Delivery, 20(2), 1325-1331.

4. Brahma S, Girgis A, (2004), Fault Location on a Transmission Line Using Synchronized Voltage Measurements, IEEE Trans. Power Delivery, 19(4), 1619-1622.

5. P.K. Dash, B.K. Panigrahi, G. Panda, (2003), Power quality analysis using S-transform, IEEE Power Delivery, vol. 18, pp. 406- 411.

6. Djuric M, Radojevic Z, Terzija V, (1998), Distance protection and fault location utilizing only phase current phasors, IEEE Trans. Power Delivery, 13(4), 1020-1026.
7. Jiang Joe-Air, Yang Jun-Zhe, Lin Ying-Hong, Liu Chih-Wen, Ma Jih-Chen, (2000), An adaptive PMU based fault detection/location technique for transmission lines Part I: Theory and algorithms, IEEE Trans. Power Delivery, 15(2), 486-493.
8. Girgis A, Hart D, Peterson W, (1992), A new fault location technique for two- and three-terminal lines, IEEE Trans. Power Delivery, 7(1), 98-107.
7. Gopalakrishnan A, Hamai D, Kezunovic M, McKenna S, (2000), Fault location using the distributed parameter transmission line model, IEEE Trans. Power Delivery, 15(4), 1169-1174.
9. Y. Lin, C. Liu, C. Chen, (2001), A new PMU-based fault detection/location technique for transmission lines with consideration of arcing fault discrimination-part I: theory and algorithms, IEEE Trans. Power Delivery, (4), 1587-1593.

*Email: truongtuananh@tnut.edu.vn